PERGAMON

Chemical Engineering Science 57 (2002) 3505–3520

Chemical Engineering Science

www.elsevier.com/locate/ces

A description of phase inversion behaviour in agitated liquid–liquid dispersions under the influence of the Marangoni effect

Leslie Y. Yeo, Omar K. Matar *, E. Susana Perez de Ortiz, Geoffrey F. Hewitt

Department of Chemical Engineering and Chemical Technology, Imperial College of Science, Technology and Medicine, Prince Consort Road, London SW7 2BY, UK

Received 13 December 2001; received in revised form 17 June 2002; accepted 20 June 2002

Abstract

The influence of the Marangoni effect on phase inversion behaviour is examined by integrating a microscopic study of the drop coalescence process, in which thin film drainage in the presence of insoluble surfactant occurs, into a macroscopic phase inversion model which has been developed previously using a Monte Carlo technique. This is achieved via an immobility factor, obtained from a comparison of the film drainage times for surfactant-laden systems and surfactant-free systems as a function of the drop approach velocity, surface Péclet number, initial surfactant concentration and the Hamaker constant, which is then used to modify the coalescence probability in the phase inversion model. On the one hand, the results indicate that the Marangoni effect removes any influence that the viscosity ratio has on phase inversion due to immobilisation of the interface, thus shielding the flow in the film from the effects of the flow in the dispersed phase; the point at which phase inversion occurs therefore tends towards equivolume holdups with the addition of surfactant. On the other hand, when comparisons are made with pure systems in which surfactant is absent, the system is seen to be either stabilised or de-stabilised from inversion depending on the viscosity ratio of the system. This is attributed to the influence of surfactant on the dispersion morphologies on either side of the inversion (i.e. water-in-oil dispersions and oil-in-water dispersions) and depends on the dispersed phase holdup; the Marangoni effect is felt stronger when the dispersed phase holdup is low.

Keywords: Emulsions; Phase inversion; Drop coalescence and break-up; Surfactant; Marangoni effect; Monte Carlo technique

1. Introduction

Phase inversion is the phenomenon whereby the phases of a dispersion of two immiscible liquids spontaneously interchange under conditions determined by the properties, phase volume holdup and energy input. In the inversion process, the dispersed phase therefore inverts to become the continuous phase and the initially continuous phase inverts to become the dispersed phase. Phase inversion is commonly encountered in a wide range of industrial processes. In liquid–liquid extraction, phase inversion is highly undesirable since the design of the contacting equipment is based on a preferred direction of transfer of the solute to give optimum mass transfer rates. On the other hand, phase inversion is an integral process step in the manufacture of butter, which consists of water drops in a fat continuum, from milk, which essentially consists of fat globules in a water continuous phase.

Until now, process equipment involving phase inversion has been designed based on empirical knowledge and experience on methods of best practice. Little, however, is known about the fundamental mechanisms and parametric behaviour of the inversion process, often due to the inherent difficulty in isolating the effects of individual parameters where in many cases conflicting observations and postulations have been reported. This places a severe limitation on the design of equipment and the conditions under which the equipment can be operated.

The value of theoretically based predictions of the critical dispersed phase holdup, i.e. the point at which phase inversion occurs, cannot be underestimated as the amount of time consuming and labour-intensive experimentation required would substantially decrease with the availability of such tools. Nevertheless, there have been rather few attempts to predict the phase inversion holdup theoretically despite

* Corresponding author. Tel.: +44-20-7594-5607; fax: +44-20-7594-5604.

E-mail address: o.matar@ic.ac.uk (O. K. Matar).

0009-2509/02/$ - see front matter © 2002 Elsevier Science Ltd. All rights reserved.
PII: S0009-2509(02)00260-9

extensive research efforts. Instead, several empirical correlations have been proposed. Unfortunately, these have a limited applicability range and there has been considerable variation between their predictions for a satisfactory model to be identified (Yeo, Matar, Perez de Ortiz, & Hewitt, 2000a).

In addition, computational models developed to predict phase inversion behaviour have also been limited to date. Juswandi (1995) attempted to simulate the inversion of a dispersion of immiscible spherical drops existing in a thin liquid film flowing as an annulus around a gas core in pipeflow using a Monte-Carlo-type scheme. However, this model is limited since it does not accurately account for the actual hydrodynamics of the flow: film drainage has not been considered when accounting for drop coalescence. Although their results were suggested to be in good agreement with the experiments of Brooks and Richmond (1994b), no attempts were made to show this in detail let alone to match the experimental geometry and conditions of the flow.

This work was later modified by the authors (Yeo, Matar, Perez de Ortiz, & Hewitt, 2000b, 2002a) to predict phase inversion behaviour for liquid–liquid dispersions occurring in agitated vessels. The phase inversion process is simulated using the Monte Carlo-type technique developed by Juswandi (1995). However, a number of significant modifications are made in an attempt to account for the hydrodynamics of drop coalescence and drop break-up. In addition, a framework for allowing for drop inter-penetration, a feature that becomes increasingly prominent at high drop concentrations, to be interpreted as drop deformation is included.

Practical liquid–liquid systems of interest normally contain surface-active-agents in the form of trace contaminants accumulating at the phase interface or in the form of additives deliberately added to the dispersion. The presence of these surfactants act to alter the interfacial properties giving rise to interfacial tension gradients which, in turn, induce additional tangential interfacial stresses commonly known in the literature as Marangoni stresses. These stresses have a significant effect on the dynamics of the drops within the dispersion. Consequently, the behaviour of the phase inversion process is also altered as a result since phase inversion, widely regarded to represent the instability of the system, depends on a dynamic balance between the different hydrodynamic processes of the drop, namely, drop coalescence, drop break-up and drop deformation.

Experimental studies attempting to isolate the effect of surfactant with regards to all other physico-chemical parameters in the system are extremely difficult and therefore few such studies have been reported. The majority of these investigations mainly focus on the characteristics of the surfactant, that is, on the effect of varying the hydrophilic–lipophilic balance (HLB) on phase inversion (Brooks & Richmond, 1994a; Vaessen, 1996; Silva, Peña, Miñana-Pérez, & Salager, 1998; Zerfa, Sajjadi, & Brooks, 1999). On another front, work has also been conducted to examine the effects of inter-phase Marangoni convection due to the mass transfer of solute, a problem relevant to solvent extraction (Sawistowski, 1971; Clarke & Sawistowski, 1978; Chiang & Ho, 1996). There is, however, a lack of experimental data which investigates the influence of Marangoni effects due to adsorption of surfactant at the interface on phase inversion behaviour.

It is with this motivation that this speculative study has been conducted. Moreover, as mentioned above, the elucidation of the influence of individual physical parameters on phase inversion behaviour in isolation to one another is difficult through experimental methods. However, in a computational model, it is easy to conduct systematic parametric studies by holding all other parameters constant whilst examining the effect of varying a single parameter. In addition, whilst many investigators have suggested that a logical obvious conclusion would be that a system's tendency to invert is decreased when surfactant is present due to Marangoni effects acting to inhibit drop coalescence, we find in our simulations that this might not always necessarily be true. We postulate that although the presence of surfactants increases dispersion stability, it is possible that this is true for both sides of the inversion in cases where the surfactant's affinity for the oil and the aqueous phases are more or less equal, i.e. the surfactant stabilises both the water-in-oil dispersion as well as the oil-in-water dispersion. The critical dispersed phase holdup would then be dependent on the relative stabilities of the dispersion morphologies. It follows that the minimisation of the system's energy is a critical consideration in the modelling of the phase inversion process, an assumption not different from that of Luhning and Sawistowski (1971), Fakhr-Din (1973), Tidhar, Merchuk, Sembira, and Wolf (1986), Yeo, Matar, Perez de Ortiz, and Hewitt (2002b).

In this work, we attempt to investigate the influence of the Marangoni effect on phase inversion behaviour by incorporating a microscopic study of the thin intervening continuous phase film drainage process between two surfactant-coated drops as they approach and possibly coalesce into the macroscopic Monte Carlo technique for simulating phase inversion described above (Yeo et al., 2000b, 2002a). Recognising the limitations of the model and the dearth of experimental data against which we can validate our model, we present a predictive tool in the hope that our speculative results will give rise to further experimentation and investigation in this area.

It will be shown that the addition of surfactant can either lead to lower or higher critical dispersed phase holdups, which is somewhat contrary to suggestions made previously (Selker & Sleicher, 1965) that the presence of surfactants will always result in the stability of the system against inversion; this suggestion is directly based on the inference that if surfactant stabilises drops against coalescence, then the system will also be stabilised against inversion. The results of our speculative model suggest that this may not necessarily always be the case: the viscosity ratio is the determining factor. Specifically, we find that, for dispersed to continuous phase viscosity ratios below 1, phase inversion occurs at higher dispersed phase holdups in agreement with

previous postulations. However, if the dispersed phase is more viscous than the continuous phase, we find the reverse to be true: inversion occurs at lower dispersed phase holdups if the system is contaminated with surfactant compared to pure systems. The stability of both dispersion morphologies needs to be taken into account since the introduction of surfactant stabilises both sides of the inversion; the extent of stabilisation depends on the dispersed phase holdup.

The rest of this paper is organised as follows. The next section describes both the microscopic model for thin film drainage between two drops in the context of surfactant influenced coalescence as well as the macroscopic description of phase inversion using a Monte Carlo technique. Attention is also given to the way both models are interfaced through an immobility factor. This is followed by a discussion of the results and, finally, by the concluding remarks.

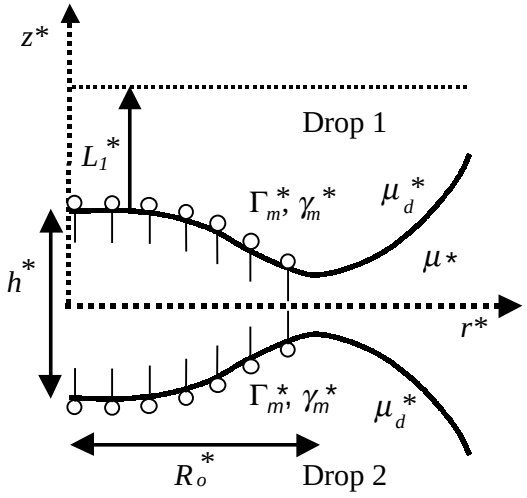

Fig. 1. Schematic representation of the drainage region of the thin intervening continuous phase film trapped between two drops.

2. Description of models

In this section, we present the multi-scale model described above, which attempts to predict the phase inversion of a liquid–liquid dispersion occurring in turbulently agitated vessels when insoluble surfactant is present at the dispersion interfaces. Although the scope is limited to agitated vessels in the present work, this model can be further generalised to other dispersed liquid–liquid systems in which the turbulence is sufficiently intense so that the collision of the drops within the system occurs by inertial impaction.

The model consists of two sub-models, a microscopic film drainage model and a Monte Carlo technique for simulating phase inversion at the macroscopic level. As such, this section will be further sub-divided into two parts. We will first briefly describe the film drainage model which will then be followed by a discussion on the Monte Carlo technique for predicting phase inversion behaviour. Only the more important details of both models are reported in this paper. The reader is referred to the previous work by the authors for the detailed derivation of the film drainage model (Yeo, 2002; Yeo, Matar, Perez de Ortiz, & Hewitt, 2002c, d) and for a more complete description of the phase inversion model (Yeo et al., 2000b, 2002a).

It should be noted that we will only consider the influence of the Marangoni effect on the drop coalescence process. The influence of the Marangoni effect on the drop break-up process is assumed to be negligible. This can be concluded by a comparison of the time scale for the drop break-up process and that for Marangoni driven spreading of surfactant at the interface. The time scale for drop break-up, T_b^*, for a drop with diameter d^* can be defined as

$$T_b^* = \frac{d^*}{\sqrt{\overline{u^{*2}}}} = \frac{d^*}{(\pi^2 N^{*3} D_I^{*2} d^*)^{1/3}} = \frac{1}{N^*}\left(\frac{d^*}{\pi D_I^*}\right)^{2/3}, \qquad (1)$$

where $\overline{u^{*2}}$ is the mean square of the relative velocity fluctuations between two diametrically opposite points on the surface of a drop (the asterisk * indicating a dimensional quantity), N^* the agitation speed and D_I^* the impeller diameter, whereas the time scale for Marangoni driven spreading of surfactant on the interface of the same drop, T_c^*, is defined as

$$T_c^* = \frac{\mu^* d^*}{S^*}, \qquad (2)$$

where μ^* is the viscosity of the continuous phase and S^* is a spreading parameter defined by $S^* = \gamma_0^* - \gamma_m^*$, where γ_0^* and γ_m^* represent the interfacial tension corresponding to the least contaminated part of the interface and that of the interfacial region saturated with surfactant at concentration, Γ_m^*, respectively. A comparison between the two time scales defined above indicates that the time scale for surfactant transport by Marangoni convection [typically $O(10^{-1})$–$O(10^{-3})$ s] could be up to three orders of magnitude larger than the time scale for drop break-up to occur [typically $O(10^{-4})$ s]. Therefore, the assumption that the influence of the Marangoni effect is negligible is justifiable within this context.

2.1. Film drainage model

2.1.1. Model description and underlying assumptions

Two spherical liquid drops which are incompressible and Newtonian, each with radius R_i^* (the label $i = 1, 2$ indicating drops 1 and 2) and initially undeformed, are considered to approach each other at constant velocity V^* along the line of their centres in the axial coordinate, z^*. The region of the draining film, also Newtonian and incompressible, is shown in Fig. 1, which depicts clearly the well-known dimpling process that accompanies film drainage. The simplifying approximations adopted in this work are as follows (Yeo et al., 2002d):

1. The liquid film in the drainage region considered is sufficiently thin, so that a small parameter ε, which defines

the relative length scales of the axial and radial dimensions, can be prescribed:

$$\varepsilon \equiv \frac{h_0^*}{R_0^*} \ll 1. \tag{3}$$

Here, h_0^* and R_0^* are the initial film thickness at $r^* = 0$ (r^* being the radial coordinate) and the initial rim radius, i.e. the radial position at which the dimple rim appears initially, respectively.

2. Both the velocity and the velocity gradient in the dispersed phase i decrease to zero over a characteristic circulation length of viscous penetration of order L_i^*, where (Li & Liu, 1996; Yeo, Matar, Perez de Ortiz, & Hewitt, 2001)

$$L_i^* = \frac{h_0^* R_i^*}{R_0^*}. \tag{4}$$

The axial pressure gradient in the dispersed phase can then be neglected compared to the radial pressure gradient since L_i^* is assumed to be small relative to the drop radius, R_i^*.

3. The effect of the variation in the drop radii on the film curvature can be neglected since $h_0^* \ll R_0^* \ll R_i^*$. Thus, symmetry relative to the plane $z^* = 0$ can be assumed and the relative drop sizes can be approximated with an equivalent radius, R^*, where

$$\frac{1}{R^*} = \frac{1}{2}\left(\frac{1}{R_1^*} + \frac{1}{R_2^*}\right). \tag{5}$$

4. Since symmetry at the plane $z^* = 0$ is assumed, we can also assume that the interfacial properties are the same at both interfaces (Lin & Slattery, 1982b; Danov, Valkovska, & Ivanov, 1999). Therefore,

$$\gamma_1^* = \gamma_2^* = \gamma^*. \tag{6}$$

γ_i^* is the interfacial tension at the interface of drop i which is a function of the interfacial concentration of insoluble surfactant, Γ^*.

5. We initially impose the presence of a dilute monolayer of insoluble surfactant with uniform concentration Γ_0^* at the film–drop interface.

6. Disjoining pressure effects in the form of van der Waals forces are considered in this model, characterised by the so-called Hamaker constant, whereas electric double layer effects are assumed to be negligible.

2.1.2. Mathematical formulation

The following transformations are applied to render the problem dimensionless:

$$r \equiv \frac{r^*}{R_0^*}, \quad z \equiv \frac{z^*}{h_0^*}; \quad h \equiv \frac{h^*}{h_0^*}, \quad p \equiv \frac{h_0^*}{S^*}p^*,$$

$$t \equiv \frac{\varepsilon S^*}{\mu^* R_0^*}t^*, \quad v_r \equiv \frac{\mu^*}{\varepsilon S^*}v_r^*, \quad \lambda \equiv \frac{\mu_d^*}{\mu^*},$$

$$R_i \equiv \frac{R_i^*}{R_0^*}, \quad \Gamma \equiv \frac{\Gamma^*}{\Gamma_m^*}, \quad \gamma \equiv \frac{(\gamma^* - \gamma_m^*)}{S^*}. \tag{7}$$

In the above scalings, h denotes the dimensionless film thickness, t is the dimensionless time and μ_d^* is the viscosity of the dispersed phase; p is the dimensionless pressure in the film whereas v_r and v_{r_i} are the dimensionless radial velocities in the film and in the dispersed phase i, respectively.

Given approximations 1 and 2, it is possible to apply the lubrication approximation both in the draining film and in the drops. Adopting a cylindrical coordinate system, we therefore write for the axisymmetric draining film

$$\frac{\partial p}{\partial r} = \frac{\partial^2 v_r}{\partial z^2}, \tag{8}$$

and for the drops,

$$\frac{\partial p_i}{\partial r} = \lambda \frac{\partial^2 v_{r_i}}{\partial z^2}. \tag{9}$$

By accounting for the tangential shear stress balance across the interfaces,

$$\left.\frac{\partial v_r}{\partial z}\right|_{z=h_1} - \lambda \left.\frac{\partial v_{r_1}}{\partial z}\right|_{z=h_1} = \frac{\partial \gamma}{\partial r}, \tag{10}$$

$$\lambda \left.\frac{\partial v_{r_2}}{\partial z}\right|_{z=h_2} - \left.\frac{\partial v_r}{\partial z}\right|_{z=h_2} = \frac{\partial \gamma}{\partial r}, \tag{11}$$

it can be shown (Yeo et al., 2001, 2002d) that the film evolution equation reads

$$\frac{\partial h}{\partial t} = \frac{1}{12r}\frac{\partial}{\partial r}\left(rh^3 \frac{\partial p}{\partial r}\right) - \frac{1}{r}\frac{\partial}{\partial r}(rhv_{r_{\text{int}}}). \tag{12}$$

The interfacial velocity, $v_{r_{\text{int}}}$, in Eq. (12) above is given by

$$v_{r_{\text{int}}} = \frac{R}{2\lambda}\frac{\partial \gamma}{\partial r} - \frac{hR}{4\lambda}\frac{\partial p}{\partial r}. \tag{13}$$

The normal stress jump condition across the interface can be expressed in dimensionless terms as (Yeo et al., 2001, 2002d)

$$p = \frac{2}{R}\frac{\varepsilon \gamma_m^*}{S^*} - \frac{1}{2}\frac{\varepsilon^2 \gamma_m^*}{S^*}\left[\frac{1}{r}\frac{\partial}{\partial r}\left(r\frac{\partial h}{\partial r}\right)\right] + \left(\Phi_\infty + \frac{B}{h^m}\right). \tag{14}$$

Here,

$$\Phi_\infty \equiv \frac{h_0^*}{S^*}\Phi_\infty^*; \quad B \equiv \frac{B^*}{S^* h_0^{*m-1}}, \tag{15}$$

where Φ_∞^* is the van der Waals interaction potential per unit volume of a semi-infinite liquid film in the limit of approaching the liquid–liquid interface, B^* is the Hamaker constant and m is a parameter. For film thicknesses below 120 Å, typical values of $B^* \sim 10^{-21}$ J and $m = 3$ have been reported (Chen & Slattery, 1982; Chen, 1985).

The dimensionless transport equation for interfacial surfactant concentration can be written as

$$\frac{\partial \Gamma}{\partial t} + \frac{1}{r}\frac{\partial}{\partial r}(rv_{r_{\text{int}}}\Gamma) = \frac{1}{Pe_s}\left[\frac{1}{r}\frac{\partial}{\partial r}\left(r\frac{\partial \Gamma}{\partial r}\right)\right], \tag{16}$$

where Pe_s is the surface Péclet number, defined by

$$Pe_s = \frac{S^* h_0^*}{\mu^* D_s^*}, \tag{17}$$

to describe the relative significance of surfactant transport due to Marangoni stresses and surface diffusion. In Eq. (17), D_s^* is the surface diffusivity. Closure of the above set of equations is achieved by a linear surfactant equation of state, justifiable for dilute surfactant concentrations (Yeo et al., 2002c, d):

$$\gamma^* = \gamma_0^* + \left(\frac{\partial \gamma^*}{\partial \Gamma^*}\right) \Gamma^*. \tag{18}$$

Since $\Gamma^* = \Gamma_m^*$ when $\gamma^* = \gamma_m^*$, it follows that

$$\left(\frac{\partial \gamma^*}{\partial \Gamma^*}\right) = \frac{S^*}{\Gamma_m^*}. \tag{19}$$

It then follows from the scaling for Γ^* that the modified interfacial tension due to the addition of surfactant reads

$$\gamma^* = \gamma_0^* - S^* \Gamma. \tag{20}$$

In dimensionless terms, the surfactant equation of state reads

$$\gamma = 1 - \Gamma. \tag{21}$$

Given that the spherical drop is initially undeformed and laden with a uniform of surfactant concentration Γ_0, the initial conditions are (Yeo et al., 2002c, d)

$$h(r, 0) = h_{00} + \frac{r^2}{\varepsilon R}, \tag{22}$$

where h_{00} is the initial film thickness at $r = 0$, and

$$\Gamma(r, 0) = \Gamma_0. \tag{23}$$

The following boundary conditions apply (Yeo et al., 2002c, d):

$$\left.\frac{\partial h}{\partial r}\right|_{r=0} = 0, \tag{24}$$

$$\left.\frac{\partial^3 h}{\partial r^3}\right|_{r=0} = 0, \tag{25}$$

$$\left.\frac{\partial h}{\partial t}\right|_{r=\infty} = -V, \tag{26}$$

$$p|_{r=r_\infty} = 0, \tag{27}$$

$$\left.\frac{\partial \Gamma}{\partial r}\right|_{r=0} = 0, \tag{28}$$

$$\left.\frac{\partial \Gamma}{\partial r}\right|_{r=r_\infty} = 0, \tag{29}$$

Table 1
Solution grid for obtaining immobility factors as a function of various parameters

Parameter	Range
V	0.01, 0.1, 1
Pe_s	1, 100, 10 000
Γ_0	0, 0.001, 0.0025, 0.01, 0.1
B	$10^{-4}, 10^{-5}, 10^{-7}$

where r_∞ denotes a radial distance far from the region in which the hydrodynamic action takes place. Due to scaling, the dimensionless approach velocity V is defined as

$$V = \frac{V^* \mu^*}{\varepsilon^2 S^*}. \tag{30}$$

2.1.3. Solution methodology

The two coupled fourth-order nonlinear parabolic partial differential equations describing the evolution of the film thickness and the surfactant concentration at the interface given in Eqs. (12) and (16) were solved numerically together with the initial conditions in Eqs. (22) and (23), and the boundary conditions given by Eqs. (24)–(29) using the Method of Lines (Schiesser, 1991; Yeo et al., 2001). We discretise the spatial domain using fourth-order centred differences and advance the solution in time using Gear's method (Matar & Troian, 1999). The solution mesh consisted of up to 1000 uniform points, convergence being achieved upon grid refinement. We halt the computations when the film thickness decreases to approximately 0.1 dimensionless units since the increasingly singular spatial derivatives in the vicinity of the rupture region became increasingly difficult to resolve accurately. In the simulations, we assume $R = 4$, $\gamma_m^* = S^* = 40$ dyn cm^{-1} and $h_{00} = 1$.

The ranges of parameters over which the immobility factor, Υ, defined by

$$\Upsilon = \frac{t_{\text{drain}}|_{\Gamma_0}}{t_{\text{drain}}|_{\Gamma_0 = 0}}, \tag{31}$$

is calculated are given in Table 1. In Eq. (31), $t_{\text{drain}}|_{\Gamma_0}$ is the time taken for the film to drain to a dimensionless thickness of 0.1 for a surfactant-laden system and $t_{\text{drain}}|_{\Gamma_0 = 0}$ is that for a pure system. These ranges have been chosen to be sufficiently wide so as to determine Υ over the full range of drainage dynamics. By repeating the simulation for the various combinations of parameters, we obtain 108 sets of immobility factors from which a correlation for the immobility factor can be regressed with respect to the various system parameters. Only the viscosity ratio between the drop phase and the continuous film phase is not included since it has been shown that the effect of viscosity ratio on film drainage is quickly diminished (Yeo et al., 2002c, d) since even very minute quantities of surfactant quickly immobilises the interface such that the flow in the drop phase is negligible on the drainage of the film. Moreover, typical values for the

surface Péclet number and the approach velocities within the turbulent flow field in the agitated vessel result in large immobility factors of order 10 such that even at very low surfactant concentrations, the interface is effectively immobilised. Therefore, in this respect, the effect of the viscosity ratio on the immobility factor can be considered negligible.

2.2. Phase inversion model

2.2.1. General approach

The Monte Carlo technique employed consists of a dispersion system with an initially uniform drop size distribution, the drop size used corresponding to the Sauter mean (i.e. the surface area to volume weighted average) diameter d_{32}. In this work, the correlation of Chen and Middleman (1967) for d_{32} was employed. The drops are initially spherical and placed in a face centred cubic configuration lattice, the dimensions of which are determined by the dispersed phase holdup and the initial drop size (Yeo et al., 2002a).

The algorithm for the model is shown in Fig. 2. For a given dispersed phase holdup and dispersion morphology, a drop is chosen at random and translated within the dispersion lattice via a method somewhat similar to the Metropolis Monte Carlo method (Metropolis, Rosenbluth, Rosenbluth, Teller, & Teller, 1953):

$$x^* \rightarrow x^* + \alpha(2\xi_1 - 1), \tag{32}$$

$$y^* \rightarrow y^* + \alpha(2\xi_2 - 1), \tag{33}$$

$$z^* \rightarrow z^* + \alpha(2\xi_3 - 1), \tag{34}$$

where x^*, y^* and z^* are the coordinates of the drops, α is an adjustable parameter governing the magnitude of the displacement and ξ_i $(i = 1, 2, 3)$ are random numbers between 0 and 1. A sensitivity analysis of α between the ranges 5% and 50% indicated that the results are largely insensitive to α and thus a value of 10% of the maximum lattice diameter was used (Yeo et al., 2002a).

To allow the model to be extended to high phase volume holdups which is common in systems undergoing phase inversion, the constraint of strict no-interpenetration of drops in the Monte-Carlo-type scheme has to be relaxed. This is because at high phase holdups, the movement of drops represented as rigid spheres becomes increasingly difficult. Since in reality, drops tend to deform allowing for greater packing fractions to be attained, the inter-penetration of drops will be interpreted as the 'deformation' of the drops in response to flow conditions and drop interactions within the agitated vessel.

The extent of 'deformation' will be determined by a probability governing the translation of a drop. This probability, Ψ, penalises for drop movements which result in large degrees of inter-penetration and is represented by (Yeo et al., 2002a)

$$\Psi = \exp\left(-\frac{E_d^*}{E_k^*}\right), \tag{35}$$

where E_d^* is the drop deformation energy and E_k^* is the total kinetic energy of the system available to deform the drops. E_d^* is given by

$$E_d^* = \gamma^* \Delta A_i^*, \tag{36}$$

where ΔA_i^* is the increase in the interfacial area as a result of the 'deformation' process. E_k^*, on the other hand, is expressed by

$$E_k^* \sim \rho_c^* \overline{u^{*2}} d^{*3}, \tag{37}$$

where ρ_c^* is the continuous phase density. Further details of the rules governing this probability of translation, Ψ, can be found in Yeo et al. (2002a).

Subsequently, the probability of the moved drop coalescing with a neighbouring drop is considered. If the resulting coalesced drop size exceeds the maximum stable drop size, $d_{\max}^*$ (given by Shinnar, 1961), it breaks up again into a drop with size $d_{\max}^*$ and a smaller drop. Another drop is then chosen at random and the possibility of it breaking up is checked (together with the possibility of the resulting daughter drops re-coalescing with other neighbouring drops).

The above steps are repeated for a large number of moves (approximately 2 00 000) such that 'steady-state' is reached where the final energy state of the system becomes largely independent of initial drop conditions. The total interfacial energy of the system is then calculated for this dispersion morphology. The whole process is then repeated for the other dispersion morphology.

The criterion for determining the point at which phase inversion occurs used here is minimisation of interfacial energy. Given that phase inversion is a spontaneous process, it is not unreasonable to assume that the total system energy content is minimised at the point of inversion (Luhning & Sawistowski, 1971) Nevertheless, since it has been found that there is always a reduction in interfacial energy at the inversion point without any measurable change in the power input being detected (Fakhr-Din, 1973), the minimisation of the total energy content of the system arises out of a redistribution between the interfacial energy and the total kinetic energy of the system. As changes in the interfacial energy are normally observed to be of the same magnitude with the total system energy, it can be concluded that the change in kinetic energy would be small compared to the change in the interfacial energy during phase inversion (Fakhr-Din, 1973). Thus, interfacial energy minimisation serves as a reasonably satisfactory criterion for phase inversion.

Phase inversion from a water-in-oil (w/o) dispersion to an oil-in-water (o/w) dispersion is thus taken to occur when the interfacial energy for the (o/w) system becomes lower than that of the (w/o) system. By determining the interfacial energies for both dispersion morphologies as a function of

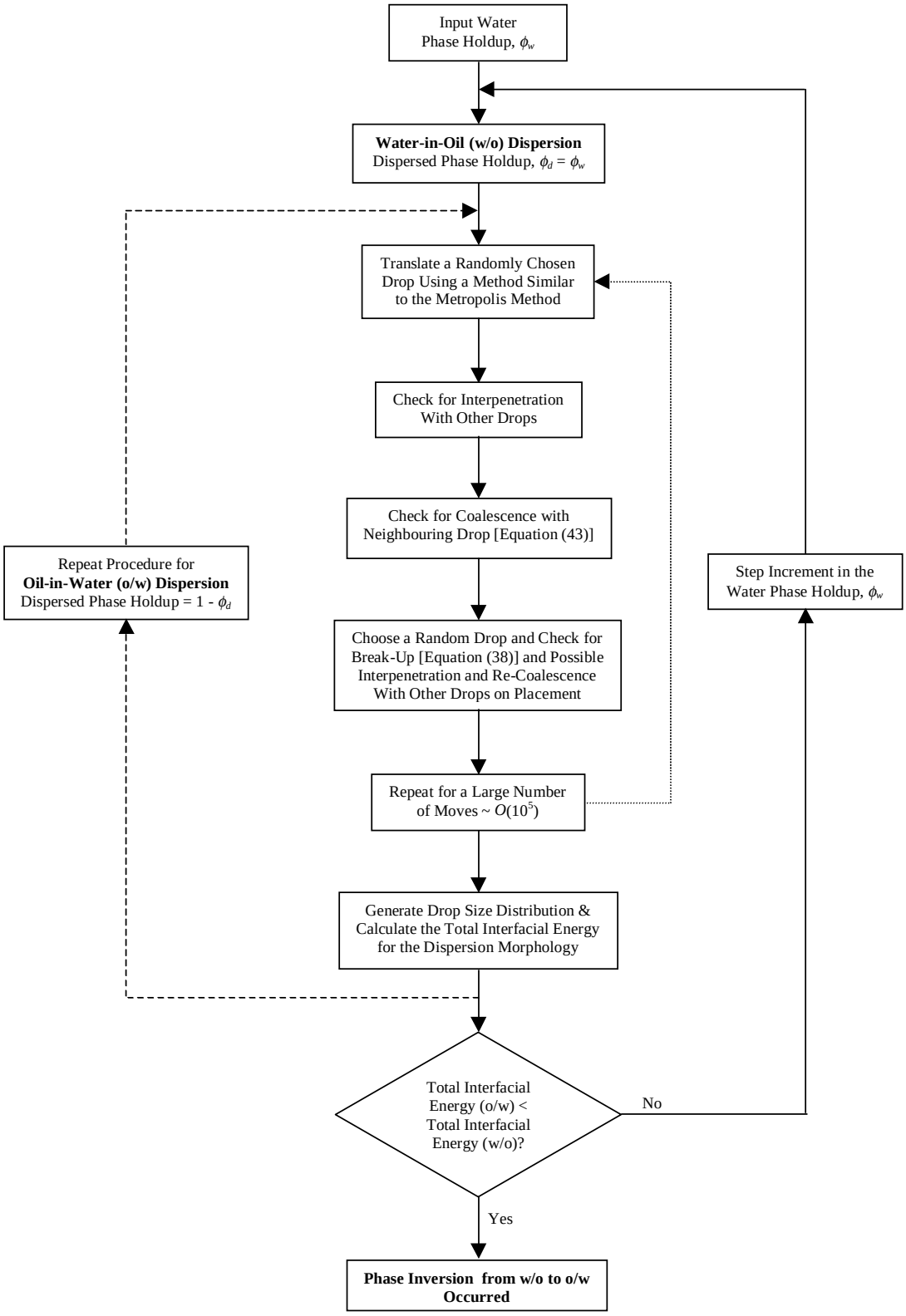

Fig. 2. Algorithm for the phase inversion model (Yeo et al., 2002a).

the dispersed phase holdup using the algorithm described above, the critical dispersed phase holdup at which phase inversion occurs can then be determined.

2.2.2. Probability of drop break-up and coalescence

The possibility of drop break-up and coalescence are considered by comparing the probability of break-up and

coalescence to a random number generated. The probability of break-up, Ω, is given as follows (Yeo et al., 2002a):

$$\Omega = \Phi\left[\exp\left(-\frac{\mu_d^*}{\mu^*}\right)\right] + (1-\Phi)\left[\exp\left(\frac{We}{We_{\text{crit}}} - 1\right)\right], \tag{38}$$

where Φ is a weighting factor to distinguish between viscous and inertial break-up, given by the ratio of the size of the smallest eddies which dissipate energy due to viscous effects to the diameter of the drop d^* for which the probability of break-up is to be evaluated on

$$\Phi = \frac{\eta^*}{d^*} \quad \text{for } \eta^* < d^*, \tag{39}$$

and

$$\Phi = 1 \quad \text{for } \eta^* \geqslant d^*. \tag{40}$$

Here, η^* is the Kolmogoroff length scale:

$$\eta^* = \left(\frac{{v^*}^3}{\varepsilon_d^*}\right)^{1/4}, \tag{41}$$

where v^* is the kinematic viscosity and ε_d^* is the turbulent energy dissipation per unit mass of fluid. In Eq. (38), We_{crit} is the critical Weber number above which drop break-up occurs (Hinze, 1955):

$$We_{\text{crit}} = \frac{\rho^* \overline{u^{*2}} d_{\max}^*}{\gamma^*}, \tag{42}$$

where ρ^* is the density.

The coalescence probability, Λ, can be obtained from two models using the following expression (Sovová, 1981):

$$\Lambda(v_1^*, v_2^*) = \Lambda_1(v_1^*, v_2^*) + \Lambda_2(v_1^*, v_2^*) - \Lambda_1(v_1^*, v_2^*)\Lambda_2(v_1^*, v_2^*), \tag{43}$$

where v_1^* and v_2^* are the volumes of the coalescing drops. Λ_1 is given by Coulaloglou and Tavlarides (1977):

$$\Lambda_1 = \exp\left[-\frac{K_1^* \mu^* \rho_c^* D_I^{*2} N^{*3}}{\gamma^{*2}}\left(\frac{v_1^{*1/3} v_2^{*1/3}}{v_1^{*1/3} + v_2^{*1/3}}\right)^4\right]. \tag{44}$$

In the equation above, K_1^* is a dimensional constant related to the film thickness at coalescence:

$$K_1^* \sim \frac{1}{h_c^{*2}} - \frac{1}{h_0^{*2}}, \tag{45}$$

where h_0^* is the initial film thickness and h_c^* is the critical film rupture thickness. Λ_2 is given by Sovová (1981):

$$\Lambda_2 = \exp\left[-\frac{K_2 \gamma^* (v_1^{*2/3} + v_2^{*2/3})(v_1^* + v_2^*)}{\rho_d^* N^{*2} D_I^{*4/3} v_1^* v_2^* (v_1^{*2/9} + v_2^{*2/9})}\right], \tag{46}$$

where K_2 is a dimensionless constant obtained through regression of experimental data and ρ_d^* the dispersed phase density.

2.2.3. Marangoni effects on drop coalescence

Since Λ_1 is a comparison between the time taken for the film to drain, t_{drain}^*, and the time that the drops spend in contact with each other, t_{contact}^*, i.e.

$$\Lambda_1 = \exp\left(-\frac{t_{\text{drain}}^*}{t_{\text{contact}}^*}\right), \tag{47}$$

we can incorporate the immobility factor Υ as a multiplier for t_{drain}^* to allow for the influence of surfactant in retarding the drainage of the film through Marangoni effects. Eq. (44) then reads

$$\Lambda_{1\Upsilon} = \exp\left[-\frac{\Upsilon K_1^* \mu^* \rho_c^* D_I^{*2} N^{*3}}{\gamma^{*2}}\left(\frac{v_1^{*1/3} v_2^{*1/3}}{v_1^{*1/3} + v_2^{*1/3}}\right)^4\right]. \tag{48}$$

In order for Υ to be calculated as a function of its parameters, V, Pe_s, Γ_0 and B, we need to evaluate these quantities given the conditions of the macroscopic system. Whilst B and Pe_s can be obtained from Eqs. (15) and (17), respectively, the dimensional approach velocity, V^*, can be found by the following expression (Kumar, Kumar, & Gandhi, 1993):

$$V^* = \frac{\frac{F^*(3+3\lambda)}{6\pi\mu^* d_{\text{mean}}^*(2+3\lambda)}}{1 + \frac{d_{\text{mean}}^*}{h_0^*}\frac{1+0.38q}{1+1.69q+0.43q^2}\frac{3+3\lambda}{2+3\lambda}}, \tag{49}$$

where F^* is the approach force given by Coulaloglou and Tavlarides (1977):

$$F^* \sim \rho_c^* \varepsilon_d^{*2/3} \frac{(d_1^* d_2^*)^2}{(d_1^* + d_2^*)^{4/3}}. \tag{50}$$

d_1^* and d_2^* are the diameters of the colliding drop pair and d_{mean}^* is the mean drop diameter defined by

$$d_{\text{mean}}^* = \frac{d_1^* d_2^*}{d_1^* + d_2^*}. \tag{51}$$

q is defined as

$$q = \frac{1}{\lambda}\sqrt{\frac{d_{\text{mean}}^*}{h_0^*}}. \tag{52}$$

In Eqs. (49) and (52), h_0^* is the initial separation between the drops measured after the translation of the drop; V is then obtained from Eq. (30). In addition, the interfacial tension is also altered due to the presence of surfactant with initial concentration Γ_0 using Eq. (20).

3. Results and discussion

3.1. Film drainage

A typical profile of the evolution of the film thickness and the surfactant interfacial concentration reproduced from Yeo et al. (2002d) is illustrated in Figs. 3(a) and (b), respectively. It can be seen that as the drops approach and the film begins to drain, the deformation caused to the interface results in the surfactant concentration being depleted. As

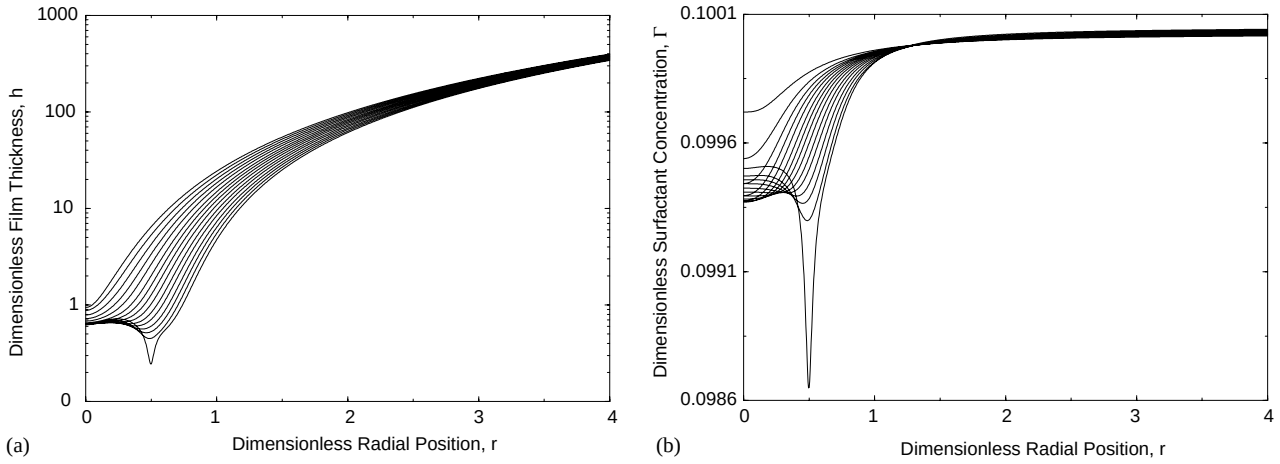

Fig. 3. Typical film thickness (a) and surfactant interfacial concentration (b) evolution profile (Yeo et al., 2002d) for 15 equal time steps up to $t = 62.2$. The remainder of the parameter values are: $\lambda = 1$, $Pe_s = 10\,000$, $\Gamma_0 = 0.1$, $B = 10^{-3}$ and $V = 0.5$.

this depletion in the deformation region continues, interfacial tension gradients arise leading to the Marangoni effect attempting to refill with surfactant. As the interface shape inverts from a convex shape to a concave shape, a dimple is formed and the rim of the dimple tends to spread outwards together with the well-like shape in the concentration profile. When van der Waals forces become significant at low film thicknesses, the film tends towards rupture in this dimple region.

Fig. 4 shows the immobilisation of the interface as surfactant is introduced to the interface. From the figure, it can be seen that the rate at which the film drains decreases quickly upon the addition of surfactant until the interface is immobilised at some value, in this case, $\Gamma_0 = 0.01$. This confirms the observations made by several investigators (Allan, Charles, & Mason, 1961; Lin & Slattery, 1982a; Klaseboer, Chevaillier, Gourdon, & Masbernat, 2000) that only a small quantity of surfactant is sufficient to immobilise the interface due to the Marangoni effect which opposes any interfacial mobility.

The film drainage times, t_{drain}, and the corresponding immobility factors, Υ, obtained from the runs generated for the various system parameters listed in Table 1 are tabulated in Tables 2–4. By regressing the data in the table to fit a nonlinear combination of the various system parameters using the least-squares fit function in *Mathematica*, we arrive at the following correlation for the immobility factor as a function of the approach velocity, surface Péclet number, initial surfactant concentration and the dimensionless Hamaker constant:

$$\Upsilon = 1 + \frac{2.194 V^{0.056} Pe_s^{0.259} \Gamma_0^{0.467}}{B^{0.125}}. \tag{53}$$

By inserting Eq. (53) into Eq. (48), the effect of surfactant at the microscopic level of film drainage in the coalescence process can then be investigated at the macroscopic level at which phase inversion of the system occurs.

3.2. Phase inversion

Figs. 5(a)–(c) illustrates the effect of surfactant concentration on the dispersed phase holdup at the phase inversion point from a (w/o) dispersion to an (o/w) dispersion, $\phi_{d,i}$, for various viscosity ratios, λ, and agitation speeds, N, for an equal density system [the effect of density on phase inversion has been discussed in an earlier work (Yeo et al., 2002a) and will not be discussed in this paper]. We have also included the set of results for pure systems in which surfactant is absent, as well as the scaling relations of Yeh, Haynie, and Moses (1964):

$$\frac{\phi_{d,i}}{1 - \phi_{d,i}} = \sqrt{\frac{\mu_d^*}{\mu^*}}, \tag{54}$$

and Arirachakaran, Oglesby, Malinowsky, Shoham, and Brill (1989), the latter relevant for phase inversion occurring in pipe flow but included here for comparative purposes.

In general, the trends for both pure and surfactant-laden systems show that the phase inversion holdup increases as the dispersed phase becomes increasingly viscous, consistent with the observations of Selker and Sleicher (1965), as well as the scaling laws given in Yeh et al. (1964) and Arirachakaran et al. (1989). At the extreme ends of the viscosity ratios, the curves tend to level off.

As the agitation in the vessel is intensified, it can be seen that phase inversion is achieved with greater ease. This is in qualitative agreement with the results of Quinn and Sigloh (1963) and with the intermediate inversion curves of McClarey and Mansoori (1978). In addition, the results also show that when there are no viscosity differences between the dispersed and continuous phases, the system inverts at equivolume holdups in agreement with the predictions in McClarey and Mansoori (1978). A detailed discussion of these general trends for the case in which surfactant is absent can be found in Yeo et al. (2002a).

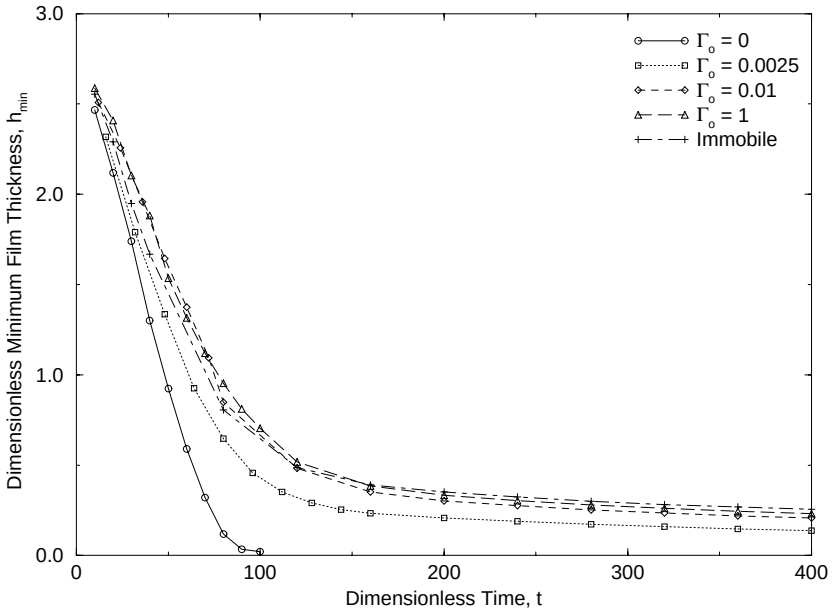

Fig. 4. Comparison of the minimum film thickness with time for the case of the surfactant-free system, surfactant-free system with immobile interfaces ($v_{r_{\text{int}}} = 0$), and for surfactant-laden systems with $\Gamma_0 = 0.0025$, 0.01 and 1 showing the immobilisation of the interfaces upon introduction of surfactant (Yeo et al., 2002d). The remainder of the parameter values are $\lambda = 1$, $B = 0$ and $V = 0.05$ and, where applicable, $Pe_s = 10\,000$.

A comparison of Figs. 5(a)–(c) shows that as the surfactant concentration is increased, the curves tend towards a horizontal line close to the line of equivolume holdup. This is because the presence of surfactant gives rise to the Marangoni effect thereby immobilising the interfaces. As a result, the flow in the dispersed phase and hence the viscosity ratio has negligible effect on the drainage of the film. Whilst this has been observed on the microscopic level in the drainage of the thin film during the drop collision process (Klaseboer et al., 2000; Yeo et al., 2002c, d), our results here show that this effect is also evident at the macroscopic level for the entire ensemble of drops within the system. The absence of viscosity ratio effects cannot be attributed to our omission of the viscosity ratio from the immobility factor as discussed in the previous section because viscosity effects are still present within the model in the break-up and coalescence probabilities [Eqs. (38) and (44)]. Therefore, it can be concluded that Marangoni effects felt at the microscopic level do indeed affect the stability of the entire system at the macroscopic dimension.

It can also be seen from the trends for each given agitation speed that the phase inversion holdup increases for $\lambda < 1$, but decreases for $\lambda > 1$ when surfactant is present for the surfactant concentrations considered. The exception to this observation is the case of extremely low surfactant concentrations and high agitation speeds ($N = 25, 40\ \text{s}^{-1}$) in which the phase inversion holdup increases for $\lambda > 1$ as seen in Fig. 5(a). This exceptional case will be dealt with at the end of this section. In general, however, the inversion process becomes increasingly difficult upon the addition of surfactant for $\lambda < 1$ and relatively easier for $\lambda > 1$. This is perhaps contrary to previous suggestions that the presence of surfactant will delay the onset of phase inversion to higher dispersed phase holdups (Selker & Sleicher, 1965). While this is a direct inference from the fact that the presence of surfactant inhibits coalescence and hence results in the stability of a dispersion, there has not been substantial experimental evidence over a wide range of viscosity ratios to validate this suggestion. Here, we suggest a possible explanation for why this may not always be true.

Since the immobility factor, Υ, is only a function of B, Γ_0, and Pe_s, and only a weak function of V, it can be shown from the definitions of these dimensionless quantities in Eqs. (15), (17) and (30), respectively, that Υ is only dependent on the initial film thickness, h_0^*, if Γ_0, S^*, λ, and N are held constant. Since h_0^* is primarily inversely proportional to the dispersed phase holdup, then it follows that Pe_s is inversely proportional to the dispersed phase holdup whereas B is proportional to it. Therefore, from Eq. (53), it becomes evident that Υ decreases as the dispersed phase holdup increases. In other words, the Marangoni effect on immobilising the interface and hence retarding drop coalescence is felt more strongly for dilute dispersions than for concentrated dispersions. The dispersed phase holdup may therefore be an important factor when considering the stability of system on a macroscopic level.

For $\lambda < 1$, phase inversion from a (w/o) dispersion to an (o/w) dispersion occurs at dilute (w/o) concentrations when surfactants are absent. Therefore, the (w/o) dispersion morphology is generally dilute whereas the corresponding (o/w) dispersion is concentrated and hence the Marangoni effect would retard coalescence to a greater extent for the

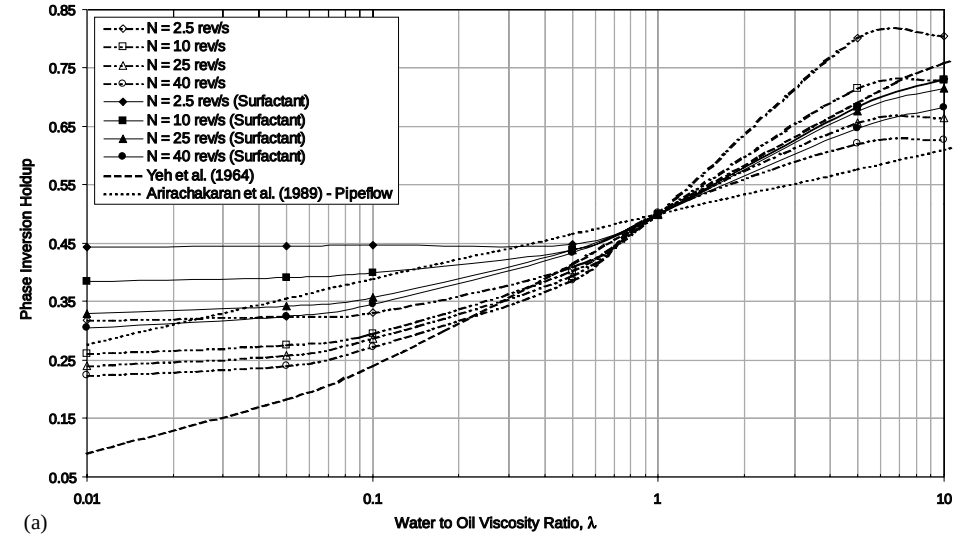

(a)

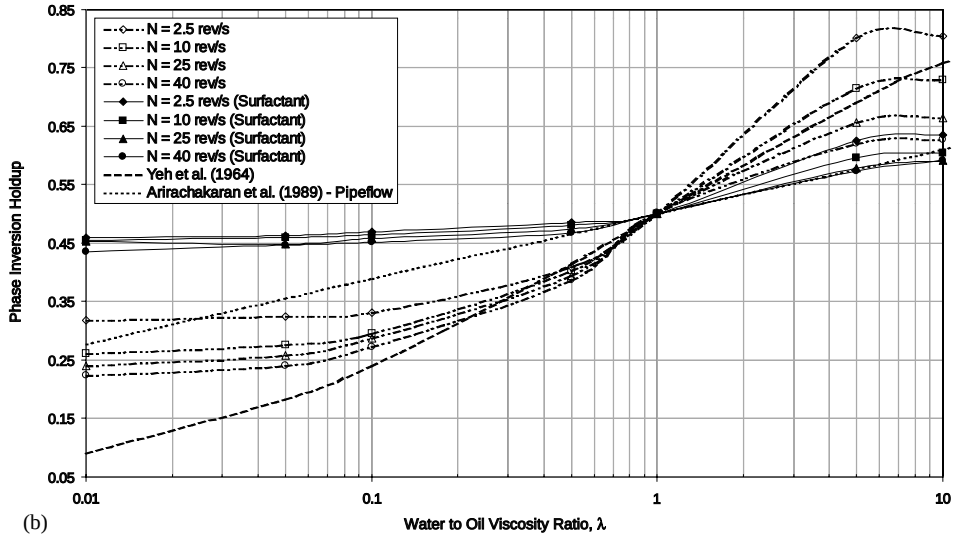

(b)

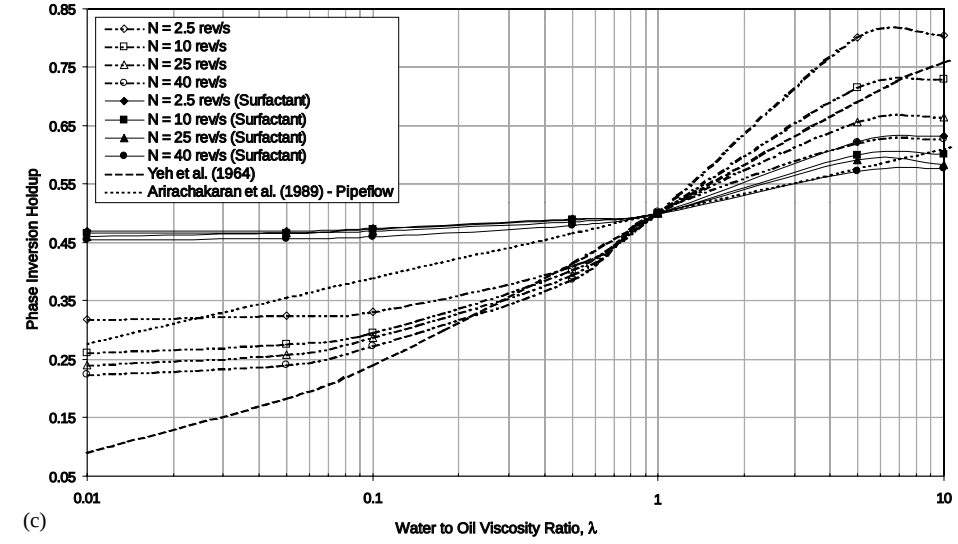

(c)

Fig. 5. Effect of water-to-oil viscosity ratio on inversion holdup for an equal density system for three initial surfactant concentrations: (a) $\Gamma_0 = 0.0001$, (b) $\Gamma_0 = 0.01$, and (c) $\Gamma_0 = 0.1$ (note that the lines were added to aid clear viewing of the trends rather than on a theoretical basis).

Table 2
Film drainage times and immobility factors as a function of various parameters for $V = 0.01$

Pe_s	Γ_0	B	t_{drain}	Υ
—	0	10^{-4}	62.05	—
		10^{-5}	83.60	—
		10^{-7}	128.49	—
1	0.001	10^{-4}	62.09	1.0006
		10^{-5}	91.27	1.0917
		10^{-7}	138.01	1.0741
1	0.0025	10^{-4}	68.61	1.1057
		10^{-5}	98.00	1.1722
		10^{-7}	139.95	1.0892
1	0.01	10^{-4}	77.47	1.2487
		10^{-5}	106.32	1.2718
		10^{-7}	140.05	1.0900
1	0.1	10^{-4}	99.10	1.2972
		10^{-5}	108.94	1.3031
		10^{-7}	143.52	1.1170
100	0.001	10^{-4}	65.05	1.0476
		10^{-5}	104.00	1.2440
		10^{-7}	143.20	1.1145
100	0.0025	10^{-4}	69.33	1.1174
		10^{-5}	104.92	1.2550
		10^{-7}	151.00	1.1752
100	0.01	10^{-4}	84.70	1.3651
		10^{-5}	134.50	1.6193
		10^{-7}	183.51	1.4282
100	0.1	10^{-4}	117.72	1.8972
		10^{-5}	217.33	2.5997
		10^{-7}	260.00	2.0235
10 000	0.001	10^{-4}	111.34	1.7943
		10^{-5}	167.16	1.9995
		10^{-7}	244.95	1.9064
10 000	0.0025	10^{-4}	119.72	1.9294
		10^{-5}	226.10	2.7045
		10^{-7}	521.25	4.0567
10 000	0.01	10^{-4}	157.00	2.5302
		10^{-5}	324.00	3.8756
		10^{-7}	3762.50	29.2824
10 000	0.1	10^{-4}	177.13	2.8546
		10^{-5}	444.79	5.3205
		10^{-7}	7196.40	56.0075

Table 3
Film drainage times and immobility factors as a function of various parameters for $V = 0.1$

Pe_s	Γ_0	B	t_{drain}	Υ
—	0	10^{-4}	20.10	—
		10^{-5}	29.40	—
		10^{-7}	46.86	—
1	0.001	10^{-4}	21.10	1.0498
		10^{-5}	29.47	1.0017
		10^{-7}	46.94	1.0009
1	0.0025	10^{-4}	21.15	1.0522
		10^{-5}	29.49	1.0023
		10^{-7}	47.11	1.0046
1	0.01	10^{-4}	21.30	1.0597
		10^{-5}	29.69	1.0092
		10^{-7}	47.54	1.0136
1	0.1	10^{-4}	30.06	1.4959
		10^{-5}	46.86	1.5928
		10^{-7}	55.31	1.1794
100	0.001	10^{-4}	22.08	1.0985
		10^{-5}	33.02	1.1225
		10^{-7}	53.83	1.1478
100	0.0025	10^{-4}	23.92	1.1901
		10^{-5}	34.09	1.1587
		10^{-7}	57.49	1.2257
100	0.01	10^{-4}	31.38	1.5614
		10^{-5}	47.72	1.6220
		10^{-7}	65.19	1.3899
100	0.1	10^{-4}	80.56	4.0080
		10^{-5}	174.65	5.9363
		10^{-7}	2482.65	52.9350
10 000	0.001	10^{-4}	26.08	1.2975
		10^{-5}	34.82	1.1836
		10^{-7}	63.47	1.3534
10 000	0.0025	10^{-4}	37.98	1.8896
		10^{-5}	35.38	1.2027
		10^{-7}	72.71	1.5503
10 000	0.01	10^{-4}	137.77	6.8542
		10^{-5}	1161.64	39.4848
		10^{-7}	1739.07	37.0804
10 000	0.1	10^{-4}	225.75	11.2313
		10^{-5}	1889.93	64.2395
		10^{-7}	2705.90	57.6951

(w/o) dispersion than for the (o/w) dispersion if all other parameters are held constant. Thus, the mean drop size for the (w/o) dispersion decreases giving rise to a larger total interfacial energy resulting in an increase in the phase inversion holdup.

The opposite is true for the case of $\lambda > 1$. It can be seen from the plots that phase inversion occurs at large (w/o) concentrations for pure systems. Therefore, upon addition of the surfactant, the influence that the Marangoni effect exerts on the (o/w) dispersion is greater than that for the (w/o) dispersion resulting in a retardation of the rate of coalescence in the (o/w) system. In the same way, there is a decrease in the mean drop size for the (o/w) system and a corresponding increase in the total interfacial energy therefore making inversion from (w/o) to (o/w) easier.

For systems in which $\lambda = 1$, the morphologies are indistinguishable for an equidensity system. Therefore, the strength of influence of the Marangoni effect is the same for both (w/o) and (o/w) and hence the effect of surfactant is not apparent, the inversion holdup being held constant at 50%.

We now turn our consideration to the exception to these trends: the case in which the surfactant concentration is extremely low ($\Gamma_0 = 0.0001$) and the agitation is very intense ($N = 25, 40\ \text{s}^{-1}$). In the discussion above, we have assumed that the contribution of the approach velocity in immobilising the interface is small. However, when the agitation speeds are high and the surfactant is very dilute, it is possible that the effect of the approach velocity becomes dominant. From Eq. (30), we note that the dimensionless approach velocity is inversely proportional to h_0^{*2}, and therefore, it is not unreasonable for the trends discussed above to be reversed if the approach velocity term dominates in Eq. (53). Under these conditions, the Marangoni effect is instead felt more

Table 4
Film drainage times and immobility factors as a function of various parameters for $V = 1.0$

Pe_s	Γ_0	B	t_{drain}	Υ
—	0	10^{-4}	21.64	—
		10^{-5}	31.31	—
		10^{-7}	70.33	—
1	0.001	10^{-4}	21.66	1.0009
		10^{-5}	31.35	1.0012
		10^{-7}	70.49	1.0023
1	0.0025	10^{-4}	21.69	1.0024
		10^{-5}	31.44	1.0042
		10^{-7}	70.73	1.0057
1	0.01	10^{-4}	21.85	1.0099
		10^{-5}	31.89	1.0186
		10^{-7}	72.07	1.0248
1	0.1	10^{-4}	22.83	1.0551
		10^{-5}	32.95	1.0524
		10^{-7}	77.57	1.1029
100	0.001	10^{-4}	23.77	1.0982
		10^{-5}	35.12	1.1220
		10^{-7}	84.73	1.2047
100	0.0025	10^{-4}	24.94	1.1523
		10^{-5}	41.54	1.3266
		10^{-7}	107.20	1.5242
100	0.01	10^{-4}	28.22	1.3042
		10^{-5}	47.70	1.5234
		10^{-7}	173.41	2.4657
100	0.1	10^{-4}	215.83	9.9736
		10^{-5}	951.63	30.3907
		10^{-7}	1184.59	16.8433
10 000	0.001	10^{-4}	28.68	1.3254
		10^{-5}	41.98	1.3409
		10^{-7}	107.14	1.5234
10 000	0.0025	10^{-4}	36.70	1.6960
		10^{-5}	60.61	1.9357
		10^{-7}	133.01	1.8913
10 000	0.01	10^{-4}	400.95	18.5280
		10^{-5}	897.47	28.6639
		10^{-7}	1921.78	27.3252
10 000	0.1	10^{-4}	638.95	29.5265
		10^{-5}	1289.06	41.1708
		10^{-7}	2741.13	38.9753

strongly for concentrated dispersions than for dilute dispersions and hence the w/o dispersion would experience lower rates of coalescence compared to the o/w dispersion. Consequently, by the same reasoning given above, the phase inversion holdup from w/o to o/w then becomes more difficult, as observed.

4. Conclusions

In this paper, we have described the results of a speculative study conducted to provide insight into the influence of Marangoni effects on the phase inversion process. This is achieved by incorporating an analysis of Marangoni effects on the film drainage process during the collision and coalescence of two drops initially covered by a uniform concentration of insoluble surfactant under a constant approach velocity into a stochastic phase inversion model previously developed using a Monte Carlo technique (Yeo et al., 2000b, 2002a).

The 'interface' between the microscopic and macroscopic scales is an immobility factor which describes the drainage time of the film to rupture in surfactant-laden systems compared to that for pure systems. This is obtained by regressing the data for film rupture times acquired from the film drainage model for various system parameters such as the approach velocity, surface Péclet number, initial surfactant concentration and the Hamaker constant. The immobility factor is then integrated into the coalescence probability in the phase inversion model.

Previous investigators have deduced that if the presence of surfactant stabilises the film against coalescence, then the system would also be stabilised against phase inversion. Our results, however, suggest that this is not always necessarily the case; the above postulation is only true for systems in which the dispersed phase is less viscous than the continuous phase. On the other hand, for high dispersed to continuous phase viscosity ratios, the reverse is true, i.e. phase inversion occurs at lower dispersed phase holdups. When the dispersed and continuous phases cannot be distinguished (i.e. when the densities and the viscosities of both phases match), then the Marangoni effect does not influence phase inversion. However, in the majority of cases, the effect of surfactant tends to shift the inversion curves such that phase inversion occurs close to equivolume holdups and that the effect of the viscosity ratio on phase inversion is reduced. This is attributed to the fact that the Marangoni effect immobilises the interface such that it screens the flow in the film from the flow in the adjacent drop phase. Any effect due to differences in viscosity between the dispersed and continuous phases thus becomes negligible.

We suggest the following reasoning for the observation that the presence of surfactants can either stabilise or de-stabilise a system from inverting: at a macroscopic level, the influence of the Marangoni effect is not always the same unlike at the microscopic level where the surfactant always acts to stabilise the drops from coalescing. Since the dispersed phase holdup affects the proximity of the drops during the collision process, it follows that the Marangoni effect in retarding drop coalescence is felt more strongly for dilute dispersions than for concentrated dispersions.

In addition, we suggest that it is not sufficient to observe the stability of one dispersion morphology alone to determine phase inversion; phase inversion is rather a result of the relative stability (or instability) between the dispersion morphologies. When surfactant is present, it stabilises both dispersion morphologies, but to different extents depending on the dispersed phase holdup for the case of insoluble surfactants, examined in this paper. The crucial factor in determining the point at which phase inversion occurs is therefore the energies of both morphologies. This is the criterion by which we have attempted to detect inversion in our simulation.

Given the limitations of our stochastic model, we recognise that this study must only remain as a speculative tool. Nevertheless, we hope that the postulations made in this paper will encourage further work and experimental verification in this area of the influence of the Marangoni effect on phase inversion which carries important practical implications.

Notation

B^* Hamaker constant, J
d^* drop diameter, m
d_i^* diameter of drop i, m
$d_{\max}^*$ maximum stable drop diameter, m
d_{mean}^* mean drop diameter, m
D_I^* impeller diameter, m
D_s^* surface diffusivity, $m^2\ s^{-1}$
E_d^* energy required to deform a drop, J
E_k^* total kinetic energy of the system, J
F^* approach force, N
h^* film thickness, m
h_c^* critical film thickness, m
h_0^* initial film thickness, m
h_{00} initial film thickness at $r = 0$
K_1^*, K_2 coalescence constants
L_i^* characteristic circulation length of viscous penetration in drop i, m
m parameter in Eq. (14)
N^* impeller speed, s^{-1}
p film pressure
p_i pressure in drop i
Pe_s surface Péclet number
q parameter defined by Eq. (52)
r radial coordinate in cylindrical coordinate system
R^* equivalent drop radius, m
R_i^* radius of drop i, m
R_0^* initial rim radius of the film, m
S^* spreading parameter, dyn cm^{-1}
t^* time, s
t_{contact}^* contact time for colliding drops, s
t_{drain}^* film drainage time, s
$t_{\text{drain}}|_{\Gamma_0}$ film drainage time for a surfactant-laden system with concentration Γ_0
$t_{\text{drain}}|_{\Gamma_0=0}$ film drainage time for a pure system
T_b^* time scale for drop break-up, s
T_c^* time scale for convection, s
$\overline{u^{*2}}$ mean-square of the relative velocity fluctuations between two diametrically opposite points on the surface of a drop, $m^2\ s^{-1}$
v_i^* volume of drop i, m^3
v_r^* velocity in the radial direction, m s^{-1}
v_{r_i} radial velocity in drop i
$v_{r_{\text{int}}}$ radial component of the interfacial velocity
V^* approach velocity of drops, m s^{-1}
We Weber number
We_{crit} critical Weber number
x^* horizontal coordinate in rectilinear coordinate system
y^* vertical coordinate in rectilinear coordinate system
z^* lateral coordinate in rectilinear coordinate system or axial coordinate in cylindrical coordinate system

Greek symbols

α adjustable parameter governing size of movement in the Metropolis Monte Carlo method
γ_i^* interfacial tension at interface of drop i, dyn cm^{-1}
γ_m^* interfacial tension corresponding to the region at the interface saturated with surfactant, dyn cm^{-1}
γ_0^* interfacial tension corresponding to the least contaminated region at the interface, dyn cm^{-1}
Γ^* interfacial concentration of surfactant
Γ_m^* interfacial concentration of surfactant at saturation
Γ_0^* initial interfacial concentration of surfactant
ΔA_i^* change in drop interfacial area, m^2
ε small parameter
ε_d^* turbulent energy dissipation per unit mass, J $kg^{-1}\ s^{-1}$
η^* Kolmogoroff length scale, m
λ viscosity ratio
$\Lambda, \Lambda_1, \Lambda_2$ coalescence efficiency
μ^* viscosity of the continuous phase, cP
μ_d^* viscosity of the dispersed phase, cP
ν^* kinematic viscosity, $m^2\ s^{-1}$
ξ_i random numbers between 0 and 1 in Metropolis Monte Carlo technique
ρ^* density, kg m^{-3}
ρ_c^* density of the continuous phase, kg m^{-3}
ρ_d^* density of the dispersed phase, kg m^{-3}
Υ immobility factor
$\phi_{d,i}$ dispersed phase holdup at the phase inversion point
Φ break-up probability weighting factor
Φ_∞^* van der Waals interaction potential per unit volume of semi-infinite liquid film
Ψ probability governing the move of a drop resulting in a certain degree of drop inter-penetration
Ω probability of drop break-up

Note: When the variables defined above are rendered dimensionless, the asterisk * decoration is dropped.

References

Allan, R. S., Charles, G. E., & Mason, S. G. (1961). The approach of gas bubbles to a gas/liquid interface. *Journal of Colloid Science*, *16*, 150–165.

Arirachakaran, S., Oglesby, K. D., Malinowsky, M. S., Shoham, O., & Brill, J. P. (1989). An analysis of oil/water flow phenomena in horizontal pipes. Paper SPE 18836, Society of Petroleum Engineers, Oklahoma.

Brooks, B. W., & Richmond, H. N. (1994a). Phase inversion in non-ionic surfactant–oil–water systems—I. The effect of transitional inversion on emulsion drop sizes. *Chemical Engineering Science*, *49*(7), 1053–1064.

Brooks, B. W., & Richmond, H. N. (1994b). Phase inversion in non-ionic surfactant–oil–water systems—III. The effect of the oil-phase viscosity on catastrophic inversion and the relationship between the drop sizes present before and after catastrophic inversion. *Chemical Engineering Science*, *49*(11), 1843–1853.

Chen, J. D. (1985). A model of coalescence between two equal-sized spherical drops or bubbles. *Journal of Colloid and Interface Science*, *107*(1), 209–220.

Chen, H. T., & Middleman, S. (1967). Drop size distribution in agitated liquid–liquid systems. *A.I.Ch.E. Journal*, *13*(5), 989–995.

Chen, J. D., & Slattery, J. C. (1982). Effects of London–van der Waals forces on the thinning of a dimpled liquid film as a small drop or bubble approaches a horizontal solid plane. *A.I.Ch.E. Journal*, *28*(6), 955–963.

Chiang, C. L., & Ho, M. L. (1996). Influence of Marangoni effect upon characteristics of phase inversion. *Proceedings of the symposium on transport phenomena and applications* (pp. 81–85), (in Chinese).

Clarke, S. I., & Sawistowski, H. (1978). Phase inversion of stirred liquid/liquid dispersions under mass transfer conditions. *Transactions of the Institution of Chemical Engineers*, *56*, 50–55.

Coulaloglou, C. A., & Tavlarides, L. L. (1977). Description of interaction processes in agitated liquid–liquid dispersions. *Chemical Engineering Science*, *32*, 1289–1297.

Danov, K. D., Valkovska, D. S., & Ivanov, I. B. (1999). Effect of surfactants on film drainage. *Journal of Colloid and Interface Science*, *211*, 291–303.

Fakhr-Din, S. M. (1973). *Phase inversion and droplet size measurements in agitated liquid–liquid systems*. Ph.D. thesis, University of Manchester.

Hinze, J. O. (1955). Fundamentals of the hydrodynamic mechanism of splitting in dispersion processes. *A.I.Ch.E. Journal*, *1*(3), 289–295.

Juswandi, J. (1995). *Simulation of the oil–water inversion process*. M.S. thesis, Oklahoma State University.

Klaseboer, E., Chevaillier, J. Ph., Gourdon, C., & Masbernat, O. (2000). Film drainage between colliding drops at constant approach velocity: Experiments and modelling. *Journal of Colloid and Interface Science*, *229*, 274–285.

Kumar, S., Kumar, R., & Gandhi, K. (1993). A new model for coalescence efficiency of drops in stirred dispersions. *Chemical Engineering Science*, *48*(11), 2025–2038.

Li, D., & Liu, S. (1996). Coalescence between small bubbles or drops in pure liquids. *Langmuir*, *12*, 5216–5220.

Lin, C. Y., & Slattery, J. C. (1982a). Thinning of a liquid film as a small drop or bubble approaches a solid plane. *A.I.Ch.E. Journal*, *28*(1), 147–156.

Lin, C. Y., & Slattery, J. C. (1982b). Thinning of a liquid film as a small drop or bubble approaches a fluid–fluid interface. *A.I.Ch.E. Journal*, *28*(5), 786–792.

Luhning, R. W., & Sawistowski, H. (1971). Phase inversion in stirred liquid–liquid systems. *Proceedings of the international solvent extraction conference*, Vol. 2 (pp. 873–887). The Hague.

Matar, O. K., & Troian, S. M. (1999). The development of transient fingering patterns during the spreading of surfactant coated films. *Physics of Fluids A*, *11*(11), 3232–3246.

McClarey, M. J., & Mansoori, G. A. (1978). Factors affecting the phase inversion of dispersed immiscible liquid–liquid mixtures. *A.I.Ch.E. symposium series, no. 173*, Vol. 74 (pp. 134–139).

Metropolis, N., Rosenbluth, A. W., Rosenbluth, M. N., Teller, A. H., & Teller, E. (1953). Equation of state calculations by fast computing machines. *Journal of Chemical Physics*, *21*(6), 1087–1092.

Quinn, J. A., & Sigloh, D. B. (1963). Phase inversion in the mixing of immiscible liquids. *Canadian Journal of Chemical Engineering*, *41*, 15–18.

Sawistowski, H. (1971). Interfacial phenomena. In C. Hanson (Ed.), *Recent advances in liquid–liquid extraction* (pp. 293–366). Oxford: Pergamon.

Schiesser, W. E. (1991). *The numerical method of lines*. San Diego: Academic Press.

Selker, A. H., & Sleicher Jr., C. A. (1965). Factors affecting which phase will disperse when immiscible liquids are stirred together. *Canadian Journal of Chemical Engineering*, *43*, 298–301.

Shinnar, R. (1961). On the behaviour of liquid dispersions in mixing vessels. *Journal of Fluid Mechanics*, *10*, 259–275.

Silva, F., Peña, A., Miñana-Pérez, M., & Salager, J. L. (1998). Dynamic inversion hysteresis of emulsions containing anionic surfactants. *Colloids & Surfaces A: Physicochemical and Engineering Aspects*, *132*, 221–227.

Sovová, H. (1981). Breakage and coalescence of drops in a batched stirred vessel—II. Comparison of model and experiments. *Chemical Engineering Science*, *36*(9), 1567–1573.

Tidhar, M., Merchuk, J. C., Sembira, A. N., & Wolf, D. (1986). Characteristics of a motionless mixer for dispersion of immiscible fluids—II. Phase inversion of liquid–liquid systems. *Chemical Engineering Science*, *41*(3), 457–462.

Vaessen, G. E. J. (1996). *Predicting catastrophic phase inversion in emulsions*. Ph.D. thesis, Eindhoven University of Technology.

Yeh, G. C., Haynie, F. H., & Moses, R. A. (1964). Phase–volume relationship at the point of phase inversion in liquid dispersions. *A.I.Ch.E. Journal*, *10*(2), 260–265.

Yeo, L. Y. (2002). *Modelling of phase inversion and associated phenomena in liquid–liquid dispersions*. Ph.D. thesis. Imperial College of Science, Technology & Medicine, University of London.

Yeo, L. Y., Matar, O. K., Perez de Ortiz, E. S., & Hewitt, G. F. (2000a). Phase inversion and associated phenomena. *Multiphase Science and Technology*, *12*(1), 51–116.

Yeo, L. Y., Matar, O. K., Perez de Ortiz, E. S., & Hewitt, G. F. (2000b). Predicting phase inversion behaviour using a Monte Carlo technique. *Proceedings of the international symposium on multi-phase flow and transport phenomena* (pp. 144–151). Antalya, Turkey.

Yeo, L. Y., Matar, O. K., Perez de Ortiz, E. S., & Hewitt, G. F. (2001). The dynamics of Marangoni-driven local film drainage between two drops. *Journal of Colloid and Interface Science*, *241*, 233–247.

Yeo, L. Y., Matar, O. K., Perez de Ortiz, E. S., & Hewitt, G. F. (2002a). Simulation studies of phase inversion in agitated vessels using a Monte Carlo technique. *Journal of Colloid and Interface Science*, *248*, 443–454.

Yeo, L. Y., Matar, O. K., Perez de Ortiz, E. S., & Hewitt, G. F. (2002b). A simple predictive tool for modelling phase inversion in liquid–liquid dispersions. *Chemical Engineering Science*, *57*, 1069–1072.

Yeo, L. Y., Matar, O. K., Perez de Ortiz, E. S., & Hewitt, G. F. (2002c). The drainage and rupture of the film between colliding drops in the presence of surfactant. *Proceedings of the international solvent extraction conference* (pp. 70–76). Cape Town, South Africa.

Yeo, L. Y., Matar, O. K., Perez de Ortiz, E. S., & Hewitt, G. F. (2002d). Film drainage between two surfactant coated drops colliding at constant approach velocity. *Journal of Colloid and Interface Science*, submitted for publication.

Zerfa, M., Sajjadi, S., & Brooks, B. W. (1999). Phase behaviour of non-ionic surfactant–*p*-xylene–water systems during the phase inversion process. *Colloids & Surfaces A: Physicochemical and Engineering Aspects*, *155*, 323–337.